

BUILDING SIMULATION WITH LOCAL ENVIRONMENTAL CONDITIONS: DEFECTS INTEGRATION IN A THERMAL BUILDING MODEL

Auline Rodler^{1,2}, Sihem Guernouti^{1,2}, Marjorie Musy^{1,2}, Julien Bouyer³

¹Centre d'études et d'expertise sur les risques, l'environnement, la mobilité et l'aménagement (CEREMA), France, Nantes, France

²Institut de Recherche en Sciences et Techniques de la Ville (IRSTV), Nantes, France

³Centre d'études et d'expertise sur les risques, l'environnement, la mobilité et l'aménagement, Nancy, France

Abstract

A thermal envelope model has been developed and validated. This model has the advantage to integrate global and local defects, and therefore a refined spatial discretization has been used. This model is coupled to SOLENE-Microclimat tool (Musy et al., 2015). The entire coupling has the advantage to consider all the long wave exchanges between the studied building, the surrounding scene and the sky vault. The interreflexions between the building on which we will focus on for the integration of defects and the surrounding buildings and the urban scene are considered. Finally, the impact of the global or local defects are shown. The defects can be materials with different properties than the initially planned during the design stage, materials with different thicknesses or a lack of material.

Introduction

Among the thermal properties of the walls, the choice of the U-values has a high impact on the simulation results (Spitz et al (2012) (Borderon et al., 2013)). Asdrubali et al (2014) and the ISO E. 6946 showed that U-values can be underestimated up to 30% by calculation. For both retrofit and new buildings, self-inspection tools can be useful to detect the structural defects. Many buildings suffer from defects in the envelope, such as missing insulation, thermal bridging and cracks. During a walk-through thermography inspection, Fox et al (2016) calculated that conductivity defect (Missing or damaged insulation and cold bridging) represented a proportion of 37.2 % of thermally significant building defects. At the material scale, Aisani et al (2016) showed that the thermal resistance of insulations is significantly affected by all kinds of defects (crush, groove, sheath passage and opening). They showed that insulation panels were found to lose more than 36 % of their performance when openings represent only 0.5 % of the total insulation volume. Missing insulation and cracks are for example observed for constructions using prefabricated modules for panel buildings (Sztanyi, 2015).

Although these types of defects have an impact on the global performance of the envelope, in literature, they are commonly studied at a small scale and not considered at a building scale surrounded by a realistic environment.

In order to reduce the energy performance gap between as building's designed and as-built, the construction defects

need to be better localized and considered in the whole simulation process.

In this work, we focus on the impact of defects on the thermal behavior of a building surrounded by a realistic environment so as to assess their impact in actual operation conditions. In that view, we have implemented an envelope model that has the advantage to be able to consider two kind of defects:

- Defects effective on the entire envelope. The defect is for example materials with different thermal properties than the initially planned during the design stage.
- Defects effective on just a part of the envelope. The defect can be a localized lack of material, in order to deal with: missing or damaged insulation, groove, sheath passage and openings.

The aim of this paper is to study the impact of defects during the rehabilitation stage. That is, on site, we need to assess the impact of localized defects on the building thermal performance. If it has an impact then it needs to be corrected and a decision needs to be taken.

First, the dynamic building thermal model is presented. The envelope model is completely new and is adapted to the integration of the defects mentioned above. The validation process of the envelope model is presented in this paper. At first, the thermal wall model response is compared to an analytical solution. Secondly, the building envelope model comparison to TrnSys® is reported and a first comparison with the model is shown. Finally, the impacts of two defects are presented.

Modeling approach

The whole model used in this paper to carry out simulations is a coupling between the developed thermal model and the existing radiative functions of SOLENE-Microclimat representative of the environment.

SOLENE-Microclimat

SOLENE-microclimat (Musy et al., 2015) was first developed for an urban amenity assessment, with the possibility to take into account (Figure 1):

1. radiative transfers, including long-wave radiation;
2. conduction and storage in walls and soils;
3. airflow and convective exchanges;
4. evapotranspiration from natural surfaces like vegetation and water ponds or humidification systems;

In this paper, the radiative and convective transfers, the conduction and storage in soils and buildings will be considered. In this paper a real 3D geometry is considered, which comes from the 3D vectorial description of the BDTopo. The building model developed is presented in the next part.

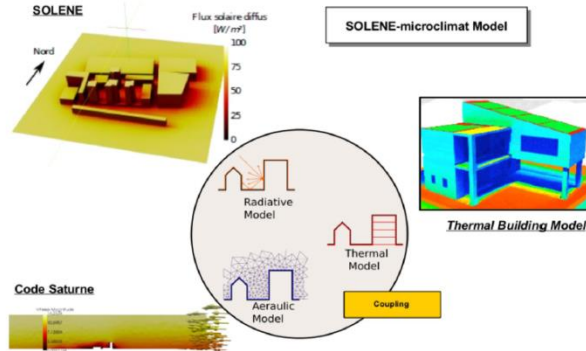


Figure 1: SOLENE-Microclimat

The wall and building thermal model

A new thermal model is developed here to answer to the aim of this paper. The only thermal model which can be coupled to SOLENE-Microclimat is the model of Bouyer et al (2012). Unfortunately, the latter is not adapted to a refined discretization of the walls as it is a 1R2C model and also the impact of the orientations of the walls on the inside surface temperatures is not considered. This model development is interesting for energy calculations of a building surrounded by a realistic environment but not when wanting to study in detail the envelope. The outputs of the latter model and the new model appear in table 1. We have decided to develop a new thermal model and not use a commercial tool as TrnSys or EnergyPlus as these tools cannot be coupled easily to SOLENE-Microclimat and also these tools do not allow to refine the spatial discretization of the walls as we expect to do.

The new model can represent the dynamic behavior of a single building of any shape using a multizone approach, where each level is a zone. Internal gains and the air exchange are considered. Heating loads are calculated as well as the air and radiant temperatures for each floor. The external surfaces temperatures are calculated for each mesh of the building, as we consider discretized boundary conditions. At the inside and for each level different surfaces temperatures for the envelope are calculated. In this thermal model, we have refined the spatial discretization of the walls. We have implemented a more detailed wall model in order to have a spatial discretization through the walls and in order to have at least a single inside surface temperature per wall and per level. Now we do not anymore connect directly the outside surface nodes to a single inside surface node but to a larger number of inside surface nodes, so that we can have several inside surface temperatures for different wall orientations. With the new model more outputs can be obtained (Table 1). Now local defects can be added and the inside surface temperatures distribution can be calculated, which was not the case before. The wall model uses a finite difference method. The spatial discretization

of the wall is flexible. For example, a mesh generator can generate finer meshes at the regions where the defect is localized. On the outside of the building envelope we have a spatial discretization according to a Gmsh unstructured triangular surface meshing (called triangles in this paper) which is also used for all the radiative calculations of SOLENE-Microclimat.

The building model is coupled to SOLENE-Microclimat tool, which has the advantage to represent the building shapes (3D geometry), the detailed external radiative exchanges, the conduction and storage in soils and the climatic environment. Between the building model and SOLENE-Microclimat we have realized a weak coupling (Figure 2). For a time step the short wave radiation after interreflection for each triangle of the urban scene is calculated. Then, the building model is run. The outside surface temperatures calculated thanks to the building model are used by SOLENE-Microclimat to calculate all the long wave and heat exchanges between the building were the thermal model is used and the soil and the other buildings of the small allotment. Finally, all the allotment's heat flows and temperatures are obtained for this time step (Figure 2).

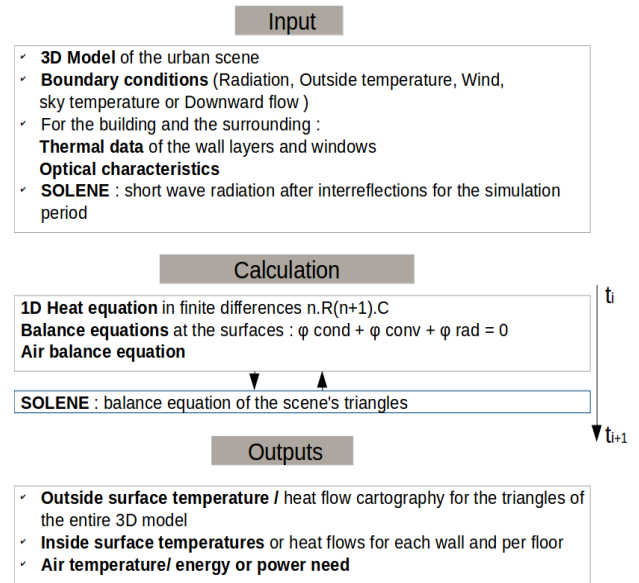


Figure 2: Calculation flow of the new thermal model coupled to SOLENE-Microclimat

Due to simulation run time constraints, in this paper we have matched for each wall the nodes located on the outside of the envelope to a single surface node exchanging with the inside of the level. That is for example, for 5 external walls we will have 5 inside surface temperatures for the walls.

Table 1: Outputs of the models

Outputs of the first model (Bouyer et al. (2012))	Outputs of the new model
For one level	For one level
<ul style="list-style-type: none"> 1 air and radiant temperature 	<ul style="list-style-type: none"> 1 air and radiant temperature Nw or more inside surface temperatures,

<ul style="list-style-type: none"> • 1 inside surface temperature for all the envelope walls • N Outside surface temperatures, where N is the number of meshes on the building envelope • 1 floor temperature • 1 ceiling temperature • Heating or cooling load 	<ul style="list-style-type: none"> • where N_w is the number of walls • N_w or more node temperatures through the wall, where N_w is the number of walls • N Outside surface temperatures, where N is the number of meshes on the building envelope • Temperature profiles through the walls • 1 floor temperature • 1 ceiling temperature • Heating or cooling load
--	--

The same is done for the roofs and windows. But for the floors, we do not apply a two dimensional discretization.

Between each level the nodes located on the flooring are the connections between the levels. For each triangle located on the building either at the inside or outside the heat equation is solved to get the triangle's temperature, T [K] :

$$\rho C_p V \frac{\partial T}{\partial t} = \Phi_{\text{conv}} + \Phi_{\text{cond}} + \Phi_{\text{SW}} + \Phi_{\text{LW}} \quad (1)$$

Here Φ_{conv} is the convective flow, Φ_{cond} is the conduction flow, Φ_{SW} is the short wave radiation flow and Φ_{LW} is the long wave radiation flow. The density of air ρ [kg/m³], the specific heat capacity C_p [J/kg K] and V [m³] the volume of the zone. The convective heat flow follows this equation

$$\Phi_{\text{conv}} = h_{\text{conv}} S_s (T_s - T_{\text{amb}}) \quad (2)$$

T_{amb} is the outside or inside air temperature, T_s is the surface temperature, S_s is the surface and h_{conv} is constant through the time for the inside of the building (6.1W/m²K for the ceiling, 1.6 W/m²K for the floor and 4.1W/m²K for the walls). For the outside, h_{conv} which will change in time, is function of the wind speed v (Jayamaha et al., 1996):

$$h_{\text{conv}} = 5.85 + 1.7 v \quad (3)$$

Here v is the wind speed [m/s].

The conduction between two neighbor meshes i and $i+1$ in the wall is given by :

$$\Phi_{\text{cond}} = k_{i,i+1} (T_i - T_{i+1}) \quad (4)$$

with

$$k_{i,i+1} = \frac{S_{i,i+1}}{\frac{\delta_i}{2\lambda_i} + \frac{\delta_{i+1}}{2\lambda_{i+1}}}$$

Here T_i [K] is a node temperature, k the thermal conductance [W/K], S [m²] the surface between two meshes, λ [W/mK] the conductivity and δ the thickness [m] between the two nodes.

Φ_{SW} [W/m²] is the shortwave radiation flow. At the inside of the building only the floor will receive radiation.

$$\Phi_{\text{SW,in}} = \alpha_{\text{SW}} \tau E_{\text{SW}} \quad (5)$$

Here, α is the absorptivity coefficient of the wall's coating, S_w is the wall's surface, τ is the solar transmission through the glaze window and E_{SW} [W/m²] the short wave radiation after inter reflection using the radiosity method. Φ_{LW} [W/m²] is the longwave radiation flow. For a triangle exposed towards the outside environment, the long wave exchanges are given by:

$$\Phi_{\text{LW,Ext,tri}} = S_{\text{tri}} \varepsilon_{\text{tri}} h_r \left(F_{\text{sky} \rightarrow \text{tri}} (T_{\text{sky}} - T_{\text{tri}}) + F_{\text{sc} \rightarrow \text{tri}} (T_{\text{sc}} - T_{\text{tri}}) \right) \quad (6)$$

Here, $h_r = \sigma (T_{\text{sky}} + T_{\text{tri}}) (T_{\text{sky}}^2 + T_{\text{tri}}^2)$ is rounded to 5 W/m²K. S_{tri} is the surface of the triangle [m²] and ε_{tri} the emissivity of the triangle. T_{sc} [K] is the temperature of a triangle of the scene, T_{tri} [K] is the temperature of a triangle of the building and T_{sky} [K] the temperature of the sky. $F_{\text{sky} \rightarrow \text{tri}}$ and $F_{\text{sc} \rightarrow \text{tri}}$ are the shape factors between the triangle considered and the sky and the shape factor between a triangle of the urban scene, a triangle of the building and the sky vault. These shape factors are directly calculated by SOLENE-Microclimat. This allows to have realistic long wave exchanges between the building studied and the surrounding. For the inside of the building, the long wave exchanges for a surface is given by :

$$\Phi_{\text{LW,Int,f}} = S_f h_r \sum_{j \neq f} \varepsilon_f F_{j \rightarrow f} (T_f - T_j) \quad (7)$$

Here S_f [m²] is the surface of the face, h_r the radiative coefficient rounded to 5 W/m²K, ε_f the emissivity, $F_{j \rightarrow f}$ the shape factor between faces, T_f the temperature of the face and T_j the temperature of another face. The finite difference equation for a node in the wall is given by:

$$\rho C_p V \frac{T_i^{t+\Delta t} - T_i^t}{\Delta t} = k_{i,i+1} (T_i^{t+\Delta t} - T_{i+1}^{t+\Delta t}) + k_{i,i-1} (T_i^{t+\Delta t} - T_{i-1}^{t+\Delta t}) \quad (8)$$

If the mesh is located on a surface:

$$\rho C_p V \frac{T_s^{t+\Delta t} - T_s^t}{\Delta t} = k_{i,i+1} (T_s^{t+\Delta t} - T_{i+1}^{t+\Delta t}) + h (T_s - T_{\text{amb}}) + \Phi_{\text{SW}}^{t+\Delta t} + \Phi_{\text{LW}}^{t+\Delta t}$$

Finally, the air temperature is given by:

$$\rho C_p V \frac{T_{\text{Air}}^{t+\Delta t} - T_{\text{Air}}^t}{\Delta t} = \sum_f h_{\text{conv}} S_f (T_{\text{Air}}^{t+\Delta t} - T_f^{t+\Delta t}) + Q + I \quad (9)$$

Where Q [W] is the heating or cooling load, I [W] is the infiltration and T_{Air} [K] the inside air temperature for a level. In this paper we consider $I = 0$.

This can be summarised as a matrix problem :

$$\mathbf{M} \begin{pmatrix} T_{\text{tri,Ext}}^{t+\Delta t} \\ \vdots \\ T_i^{t+\Delta t} \\ \vdots \\ T_{f,\text{Int}}^{t+\Delta t} \\ T_{\text{Air}}^{t+\Delta t} \end{pmatrix} = \begin{pmatrix} S_{\text{tri,Ext}} \\ \vdots \\ A_i T_i^t \\ \vdots \\ S_{f,\text{Int}} \\ A_{\text{Air}} T_{\text{Air}}^t \end{pmatrix}$$

Where $A = \frac{\rho C_p V}{\Delta t}$ and $S_{f,\text{Int}} = A_{f,\text{Int}} T_{f,\text{Int}}^t + \Phi_{\text{LW,Int,f}}$ with

$$S_{\text{tri,Ext}} = A_{\text{tri,Ext}} \cdot T_{\text{tri,Ext}}^t + S_{\text{tri}} \epsilon_{\text{tri}} h_r (F_{\text{sky} \rightarrow \text{tri}} T_{\text{sky}}^{t+\Delta t} + F_{\text{sc} \rightarrow \text{tri}} T_{\text{sc}}^{t+\Delta t}) + \Phi_{\text{SW,Ext}}^{t+\Delta t}$$

M represents the matrix coupling the entire temperatures calculated. The inversion of the matrix allows to calculate all the temperatures at the time step $t + \Delta t$ following an implicit numerical resolution method which is stable.

Validation of the building envelope model

The new envelope model has followed a validation process introduced in this paper. This is an important evolution as until now no thermal building model coupled to SOLENE-Microclimat was validated or compared to an analytical solution or commercial tool.

Comparison to an analytical solution

At first, the thermal wall model response is compared to an analytical solution. The analytical solution considers a lateral and lower adiabatic limit and a superior constant temperature $T_0 = 300$ K. The initial temperature is $T_i = 270$ K. The temporal temperature evolution for different depths z is:

$$T(z, t) = T_i + (T_0 - T_i) \text{erf}\left(\frac{z}{2\sqrt{a \cdot t}}\right) \quad (10)$$

With $a = \lambda / \rho C$ the thermal diffusivity of the material.

The response of the model in terms of temperature shows good agreement with the analytical solution calculated at $z_1 = 3.3$ mm and $z_2 = 166$ mm (Figure 3):

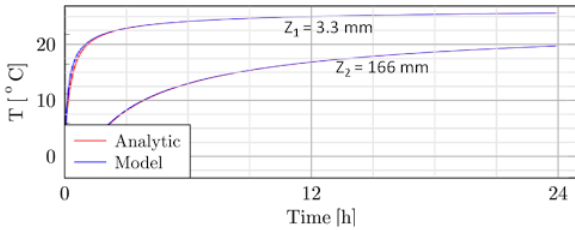


Figure 3: Wall temperature at different depths compared to an analytical solution

Comparison to TRNSYS

Secondly, the building model comparison to TrnSys® is reported. For these simulations, a simple geometry was chosen without considering the buildings for the surrounding. A 3 level cubic building was considered. The building was 30m in depth, 30m in large and 9m in height. For each floor and wall a 25 m² double-glaze window was considered. The weather data taken is shown below (Figure 4). The following assumptions were made for both TrnSys and the building thermal model:

- we have taken the same internal and external convective coefficients.
- we have assumed that the earth temperature was constant and equal to 15 °C.
- we have considered the same transmission coefficients of the windows for both direct and diffuse radiation.
- we have neglected the air infiltrations.

However, the radiation distribution between both models are different. SOLENE-Microclimat considers the sky vault as a source of diffuse energy with a non-uniform luminance distribution. TrnSys will not follow this assumption. For free floating conditions, we have compared the air temperatures for the different floors. The difference between TrnSys and the simulation can reach up to 0.8 °C and tends to be most of the time between 0.5 °C and -0.5 °C (Figure 5).

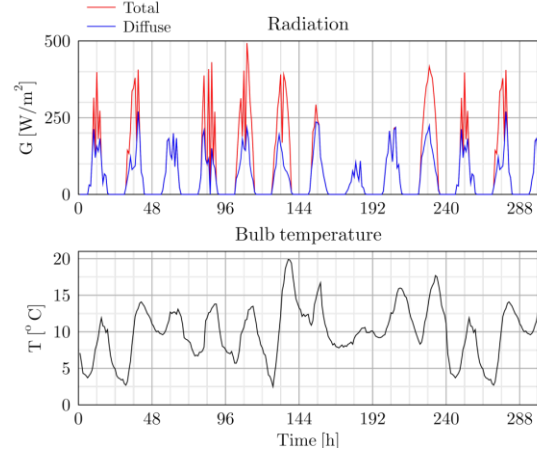


Figure 4: Weather data considered for the simulations

The highest differences are observed for the last floor.

For Winter conditions with a constant set point temperature of 19°C, the air temperatures between both tools for each floor were quite close. Differences between 0 and 0.8 °C were observed for the ground floor. The heating energy difference obtained for the ground floor represented 0.5 %, which is a very low difference. For the second floor, the air temperature difference was between 0 and 0.9°C and the heating energy difference was of 3.6 %. For the last floor the air temperature difference was again between 0 and 0.9 °C and the heating energy difference was of 4%. The global tendency of the new model is acceptable, when comparing it to either the analytical solution or TrnSys.

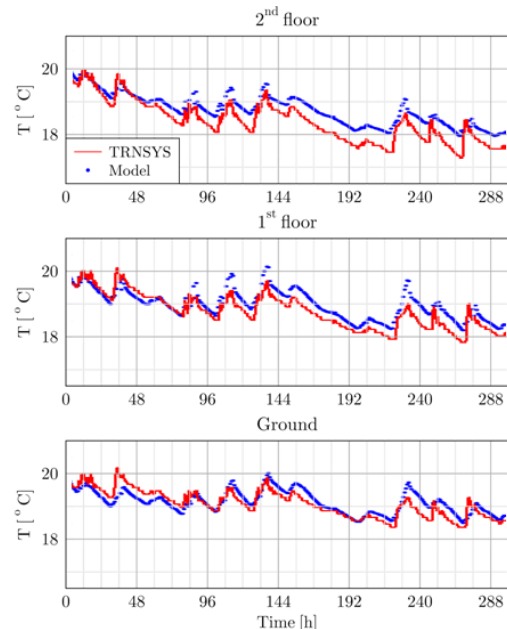


Figure 5: Air temperature of TrnSys and the model presented

Study of the defects

During the rehabilitation stage, we tend to add an exterior insulation layer on the envelope. In this paper, we will study the impact of two defects concerning the exterior insulation:

- a different insulation than the initially planned: the range of conductivity can be different and the thickness too.
- a lack of insulation.

For these studies we have considered a 5 level building which is located in Nantes. This building is surrounded by other 7 buildings belonging to the same town site. For the simulations, we considered only the central building and the four buildings surrounding it (Figure 6).

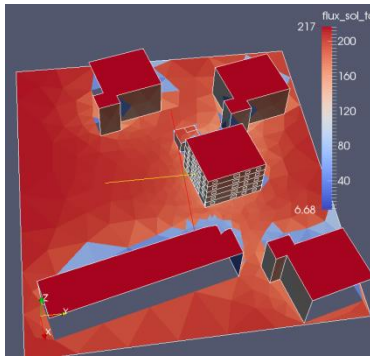


Figure 6: The urban area and the solar total radiation distribution

During this period a set point temperature of 19°C was kept constant. Here, the external walls are composed from the outside towards the inside of : a 1 cm coating, an external thermal insulation, 25 cm of concrete and 1.3 cm of plaster. The roof is considered to have the same thermal properties and thicknesses as the walls. The ground slab is composed of a 10 cm external insulation and 30 cm of concrete. Each floor is composed of 15 cm of concrete and a 1cm parquet floor (Table 2). The thermal characteristics are given below:

Table 2: Envelope thermal properties

	Coating	Insulation	Concrete	Plaster	Parquet
Conductivity (W/mK)	0.75	0.032±0.012	1.33	0.42	0.13
Density (kg/m³)	1450	30	2300	1200	1880
Heat capacity (J/kgK)	1000	1000	880	850	400

Impact of conductivity and insulation thickness differences at a whole building scale

The first type of defect we are treating is: a material with different properties than the initially planned during the design stage, material with different thickness than the initially planned or a completely new insulation type with a different property and even thickness. Simulations have been carried out to check how these defects influence the heating load. Here, the changes are made on the entire

envelope. The aim is to compare to a reference or required power associated with an uncertainty range due to the impact of the defects. Here the reference is simulation S2 (Table 3): we consider that the required exterior insulation for the rehabilitation corresponds to a 18cm thick woolen insulation where the conductivity is supposed to be 0.03 W/mK. In order to consider a defect where the thickness of the insulation might have changed simulation 1 was done. To consider the impact of both a change in thickness conductivity for a same type of insulation simulation three to six were done. Finally, for a defect where the insulation type is different than the one planned, simulation 7 to 10 were done. Here two insulation types are considered : woolen and polyurethane. The simulations are summarized in Table 3.

Table 3: Tested thicknesses and conductivity values

Simulation	S ₁	S ₂	S ₃	S ₄	S ₅	S ₆	S ₇	S ₈	S ₉	S ₁₀
Thickness [cm]	15	18	15	18	15	18	10	14	10	14
Conductivity [W/mK]	0.03	0.03	0.04	0.04	0.045	0.045	0.022	0.022	0.03	0.03
Insulation type	Woolen						Polyurethane			

For the entire envelope surface either the conductivity or the thickness was changed but not the heat capacity and density. The thicknesses were chosen according to the most commonly used for external insulation. The conductivity and thickness interval have been chosen according to the informations found in a construction report¹.

In this paper, no global sensitivity study has been done before studying the impact of the thickness and the conductivity because a large number of studies showed that among the variables identified on a building the most influential in sensitivity analysis are the U values (Borderon et al., 2013) (Spitz et al, 2012).

The uncertainty range relative to the woolen insulation is presented as the blue area on figure 7. The uncertainty range linked to the polyurethane is presented in brown (fig 8). The black curve is simulation two, considered as the reference simulation, S2.

We can see on figure 7 and 8 that between the levels the mean heating power is different. For the ground floor and last floor the demands are higher. For these cases the levels have a higher envelope surface in contact with low temperatures. The other levels which are in contact with an upper and lower floor have lower heat losses and therefore lower heating demands. These observations show that the coupling between floors works and has an impact on the powers but also on the simulations range.

The air temperature during the day can overpass the set point temperature due to the solar gains. Only at the ground floor this is not observed.

Concerning the impact of conductivity and thickness we see that the simulation range in blue and brown are higher for the ground floor and the last floor due to a higher temperature gradient between the inside and outside. The

¹ GUIDE DES MATÉRIAUX ISOLANTS pour une isolation efficace et durable :

http://www.energievie.info/sites/default/files/documents/energievie_guide_isolants_24p_bd_6.pdf

impact of conductivity and thickness of either the woolen insulation or polyurethane on the reference simulation S2 seem to be similar, unless for the ground and first floor (fig 7 and 8). In terms of energy, we have quantified the maximal absolute difference between the maximum and minimum energy obtained with the simulations of each type of insulation and with respect to simulation S2 (Table 4). We observe as expected important differences in terms of energy comparing the simulations to the reference simulation S2 for all floors and whatever the type of

Table 4: Simulation differences (normalized by the reference heat energy)

Level	Ground	1st	2 nd	3 rd	4 th
Woolen	49.7 %	56.8 %	63 %	56.6 %	55 %
Polyurethane	18.9 %	40.6 %	57.7 %	56.4 %	55 %

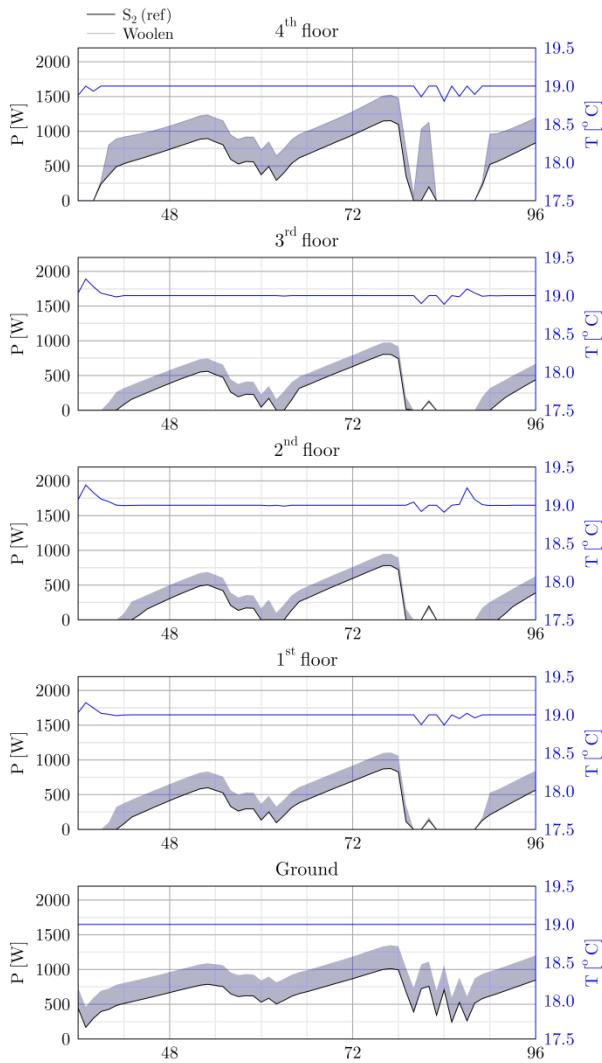


Figure 7: Heating power and air temperature for the different levels (woolen)

insulation taken. The difference is between 18.9 and 63%. The simulation bar in blue or red for either the woolen or the polyurethane are quite similar as shown on figure 10. Simulation 2, represented as the dot is often in the lower part of the error bar.

More specifically, the impact of the three defects will be discussed in detail hereafter. All simulations are compared to simulation S2 (Table 5).

We are going to evaluate the difference in terms of energy between simulation S1 and S2, in order to conclude on the impact of changing the thickness on the woolen insulation for this case study.

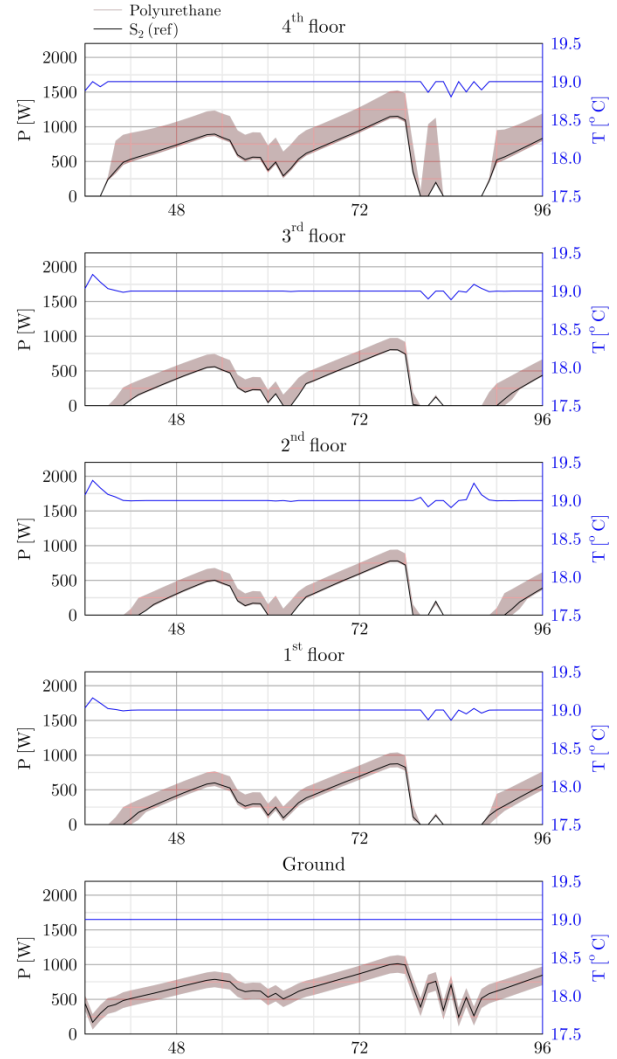


Figure 8: Heating power and air temperature for the different levels (polyurethane)

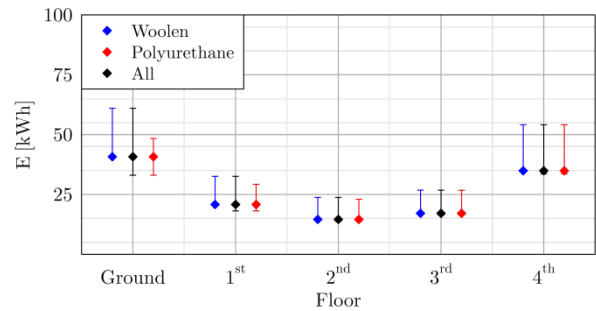


Figure 9: Energy consumption of each floor and the variation range due to the impact of conductivity and thickness

Then, we will show the difference for a change of conductivity of the woolen insulation. Therefore, we will quantify the energy difference between simulation S6 and S2. Finally, we will quantify the difference between simulation S5 and S2 for a change of both thickness and conductivity (Table 5).

Table 5: U value and Energy differences normalized by the reference heat energy between each simulation and S2

Simulation	S ₁	S ₆	S ₅	S ₇	S ₈	S ₉	S ₁₀
U [W/m ² K]	58.7	67.9	74.0	59.8	49.8	71.6	60.8
Difference [%]	11.9	38.5	56	16.0	9.12	45.7	16.2

For a change in material we will focus on simulations S7 to S10 and quantify the difference between these simulations and the reference simulation (Table 5).

We can see that for this case study, the energy difference for the first defect is the lowest. A change in terms of thickness of 3cm leads to a mean difference for the whole building of 11.9% when the U value of the global envelope is of 53W/m²K for S2 and of 58.7 W/m²K for S1. The conductivity change seems to be more important than this thickness change for this case study, as mean differences of 38.5% are observed. Of course, a change of both conductivity and thickness leads to higher mean differences, of 56.2%.

For the third defect, we supposed that polyurethane instead of woolen insulation was chosen. We see that the difference is in the range of 16 – 45.7 % depending on the thickness and conductivity value. The highest difference is observed for a thickness change, reaching 45.7%. We observe similar differences for S7 and S10. We can not conclude here on whether the thickness impacts more than the conductivity. Moreover, it is simulation S8, which is the closest to S2, for which neither the thickness nor the conductivity is the same as S2, but the U is the closest.

The air temperature differences of the different floors are not presented here as very low differences are observed. We have also observed that the differences on the outside temperature surfaces between the simulations were quite low. For the inside surfaces temperatures the differences were more important, but reached only 0.2 - 0.3 °C.

We have observed in this first application high differences among the energies when changing the conductivity, the thickness or both. Here all simulations showed important differences compared to simulation S2. These kind of defects are a source of the energy performance gap between as building's designed and as-built and would need to be corrected on site.

These defects can be located on the whole envelope or can just be part of the envelope surface. This is the reason why we have adapted the model so that it can consider local material heterogeneities or defects. This will be presented in the next application.

Impact of a local defect or heterogeneity

In case of a local defect, we can localize it on the envelope and adapt the spatial discretization of the faces of the

defect and the faces around. The defect considered here is surrounded by a red square in the figure below (Figure 10). On the ground floor we have two defects, on two different walls. We will focus on the defects located only on the ground floor. The walls have the same properties than simulation S2 in table 2. Here the defect is a lack of insulation. We have considered again simulation S2 as our reference and here the simulation with the defect is compared to simulation S2 when wanting to quantify the impact on the energy performance.

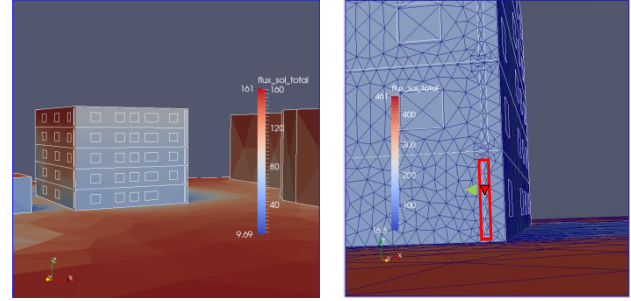


Figure 10: At the left, the building studied and at the right, a zoom on the defect of the ground floor

To add a defect in the geometry, we generate a new face (distinguished here by the white edges) which here is a rectangle but can be of any shape. Here both defects have a size of 0.4 m² for a wall of 53 m², which represents a ratio of 0.48 % between the defects' surface and the envelope surface of the ground floor. The simulations undertaken are as before for winter conditions with a heating system. We have compared the surfaces temperatures at the inside and outside of the wall for both a triangle in the defect (red triangle) and one located on the wall just beneath the defect (green triangle) (Figure 10). We observe a very small difference between the defect and the wall for the outside temperatures but a higher difference for the inside temperature (Figure 11). Up to 2.5 °C difference for the triangle in the defect and a triangle just beneath but not included in the defect is observed for the inside surface temperature. On the other hand, a maximum of 0.5°C difference is observed for the outside surface temperature (Figure 11).

We can see on the temperature profile (Figure 12) the temperatures for the different nodes through the wall. We observe again that a very low difference is observed for the first node, that is for the outside surface temperature. For the last nodes, that is the inside surface temperature we observe a difference of 2 °C.

In terms of energy consumption when considering the defect and when considering no defect (that is, simulation 2 in Table 2) the energy difference is of 2.8 %. Here the surface ratio between the defects and the envelope walls of the ground floor is of 0.48 %. In this case study, that is for an envelope with an exterior insulation and a local defect, we observe that the local defect can be visualized only on the inside of the building and this is interesting to know if wanting to use an infrared camera.

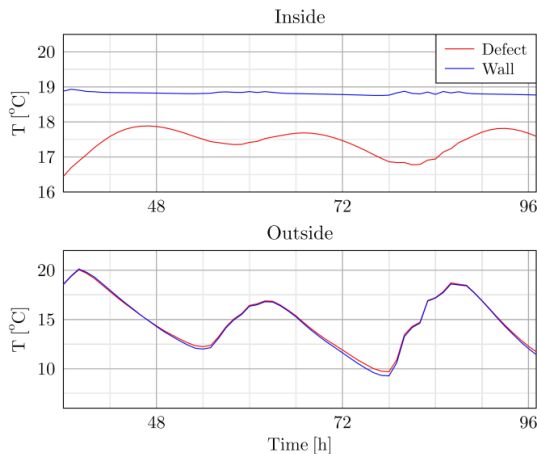


Figure 11: Single inside and outside surface temperature of the defect and the wall

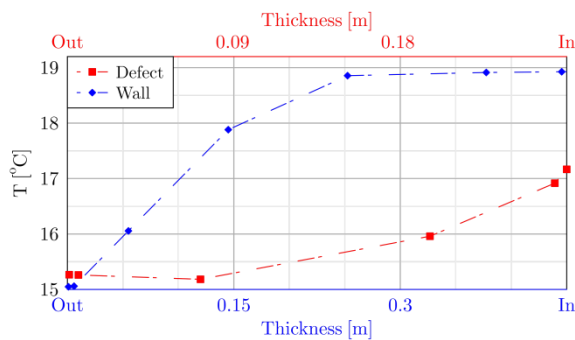


Figure 12: Temperature profile through the defect and the wall

Conclusions

An envelope model for studying defects impacts has been implemented. The defect considered here are: materials with different properties or thicknesses than the initially planned during the design stage on the entire envelope or a local defect like a lack of insulation. The model has been presented and a comparison to TrnSys showed the general coherence of the model. The coupling of the model with Solene-Microclimat has permitted to study the impact of defects for a realistic environment. First applications showed the capability of the model to integrate the defects we wanted to consider. For the first type of defects located on the entire envelope, we observed that the heating power is very sensitive to both the conductivity and thickness of the chosen insulation. For the second application, when considering a local insulation lack, we observed for winter conditions, a high impact on the inside surface temperature and a low impact on the heating power and energy, as the defect's size was small. Simulations for other periods of the year will be done in order to see where we should place the camera to localize the defects. Also more simulations need to be done to see the impact of the defect as a function of the size of the defect itself in respect to the entire surface of the walls. In future, the thermal simulation will be done starting from

infra red images and detected defects localized with these images.

Acknowledgement

This research work is carried out within the Built2Spec project (637221 – H2020-EeB-2014-2015).

References

- Aïssani, A., Chateauneuf, A., Fontaine, J.-P., Audebert Ph. (2016). Quantification of workmanship insulation defects and their impact on the thermal performance of building facades. *Applied Energy* 165 : 272–284
- Asdrubali, F. , D'Alessandro, F. , Baldinelli, G. , Bianchi, F (2014). Evaluating in situ thermal transmittance of green buildings masonries—a case study, *Case Stud.Constr. Mater.* 1 (2014) 53–59.
- Borderon, J., Lahrech, R., Millet, J.-R., Tasca-Guernouti, S. (2013). Influence of fields data quality on the modeling of residential buildings with dynamic simulation tool. 13th Conference of International Building Performance Simulation Association, Chambéry, France, August 26-28
- Bouyer, J. , Inard, C. , Musy, M. (2011). Microclimatic coupling as a solution to improve building energy simulation in an urban context, *Energy Build.* 43 (2011) 1549–1559.
- Fox, M., Goodhew, S., De Wilde, P. (2016). Building defect detection: External versus internal thermography. *Building and Environment*, 105: 317-331
- ISO, E. 6946. (2007). Building components and building elements. Thermal resistance and thermal transmittance. Calculation method, 2007.
- Jayamaha, S.E.G., Wijesundera N.E., Chou S.K., Measurement of the heat transfer coefficient for walls, *Building and Environment*, 31 (1996) 399-407.
- Musy, M., Malys, L., Morille, B., Inard, C. (2015). The use of Solene-Microclimat model to assess adaptation strategies at the district scale. *Urban Climate* 14, 213-22.
- Spitz, C., Mora, L., Wurtz, Arnaud, J. (2012). Practical application of uncertainty analysis and sensitivity analysis on an experimental house. *Energy and Buildings* 55, 459-470.
- Sztanyi Robert (2015). Construction defects in the subsequent insulation of panel buildings. Fascicle of Management and Technological Engineering, Annals of the oradea University.
- TRNSYS (1996). TRNSYS Mathematical reference.Solar Energy Laboratory Madison, United States, University of Wisconsin